Supporting Information:

Mid-infrared surface waves on a high aspect ratio nano-trench platform

Osamu Takayama,[1] Evgeniy Shkondin,[1,2] Andrey Bodganov,[3] Mohammad Esmail Aryaee Panah,[1] Kirill Golenitskii,[4] Pavel Dmitriev,[3] Taavi Repän,[1] Radu Malureanu,[1] Pavel Belov,[3] Flemming Jensen,[2] and Andrei V. Lavrinenko[1,]*

[1]DTU Fotonik—Department of Photonics Engineering, Technical University of Denmark, Ørsteds Plads 343, DK-2800 Kgs. Lyngby, Denmark

[2]DTU Danchip—National Center for Micro- and Nanofabrication, Technical University of Denmark, Ørsteds Plads 347, DK-2800 Kgs. Lyngby, Denmark

[3]International Research Centre for Nanophotonics and Metamaterials, ITMO University, St. Petersburg, Russia

[4]Ioffe Institute, Russian Academy of Sciences, 194021, St. Petersburg, Russia

Corresponding Author

*Email- alav@fotonik.dtu.dk

KEYWORDS ---

hyperbolic metamaterial, Dyakonov surface waves, metamaterial, plasmonics

1. Fabrication Procedure

1-A. Si Template fabrication

The whole fabrication work took place in a class 100 cleanroom. First, standard double side polished Si (100) wafers were selected and RCA cleaned. Conventional deep-UV lithography (DUV stepper: Canon FPA-3000 EX4) was implemented for defining the grating patterns (lines 200 nm wide and 400 nm pitch) on 2×2 cm^2 scale chips. The normal procedure includes bottom antireflective coating (BARC) and photoresist spinning, followed by spray developing. To promote adhesion and to minimize interference effects, the substrate surface was coated with a 65 nm thick BARC coating (DUV42S-6, Brewer Science, USA) followed by a bake-out at 175 °C for 60 s. The positive photoresist (KRF M230Y, JSR Micro, NV) was spin-coated to a thickness of 360 nm and baked at 130 °C for 90 s. Thereafter, deep reactive ion etching (DRIE) was used to fabricate trenches in the silicon substrate with a depth of 3 μm.

Table S1. Recipe for DRIE Bosch process.

		Passivation (1.5 s)	Etching (2.5 s)
Process gas flow (sccm)	C_4F_8	50	20
	SF_6		60
	O_2		5
Powers (W)	Coil	600	400
	Platen		40

1-B. Deep reactive ion etching (DRIE)

Three main steps were used in the Si template fabrication: etching of the BARC layer, high anisotropic silicon etching and resist removal. The BARC etch proceeds for 1 min using 40 sccm O_2 plasma with coil and platen powers of 200 and 20 W, respectively. DRIE etching (DRIE-Pegasus from SPTS) proceeds in a switched process (Bosch process) consisting of cyclic steps of etching and surface passivation, with a process pressure of 10 mTorr. The processing substrate temperature was kept at 0 °C. Table S1 summarizes the Bosch process parameters. The trench depth was controlled by adjusting the number of cycles (150 cycles corresponds to 3 μm deep trenches). The last step in Si trench fabrication is the removal of the remaining resist. It was done by using O_2 plasma for 2 min with a gas flow of 100 sccm. The coil and platen powers were 800 and 20 W, respectively. The shape of the produced Si-template trench structures was carefully investigated by SEM in cross-sectional mode by sacrificing some of the prepared structures [Figure S1a]. Prior to the next step (ALD deposition) the prepared template structure received additional O_2/N_2 plasma treatment in order to remove any possible organic residuals from resist coatings and surroundings.

1-C. Atomic Layer Deposition (ALD)

The AZO coatings were made in a thermal, hot-wall ALD system (Picosun R200). The precursors were obtained from Strem Chemicals. ZnO was deposited using diethylzinc (Zn $(C_2H_5)_2$, DEZ) and deionized water (DIW, H_2O), whereas Al doping of the ZnO was introduced by a single cycle of trimethylaluminium ($Al(CH_3)_3$, TMA) and DIW into a ZnO matrix made by 20 cycles of "DEZ +DIW". This defines an AZO macrocycle: 20 cycles of "DEZ+DIW" and one cycle of "TMA+DIW". The deposition temperature was kept constant at 200 °C. The ALD recipe for deposition of one AZO macrocycle on the Si trench template structure is presented in Table S2. The deposition results are visualized in the SEM image in Supplementary Figure S1b. Approximately 55 AZO macrocycles need to be deposited in order to fill the Si trench template entirely.

Table S2. Recipe for one macrocycle of AZO (200 °C).

Precursor	Number of repetitions	Carrier gas flow (sccm)	Pulse time (s)	Purge (s)
DEZ		150	0.1	0.5
DEZ		150	0.1	20
H_2O	20	200	0.1	0.5
H_2O		200	0.1	20
TMA		150	0.1	0.5
TMA		150	0.1	20
H_2O	1	200	0.1	0.5
H_2O		200	0.1	20

1-D. Top layer removal and selective etch of the Si template

In order to get rid of the deposited top layer of AZO and to gain access to the Si template core, a pure physical etching with Ar^+ ions (Ionfab 300 plus from Oxford Instruments) was used. Here, the process was tuned to an etch rate of 20 nm/min which provided a well-controlled top layer breakthrough [see Figure S1c]. Following this, the subsequent selective silicon etching (template removal) proceeded using a continuous isotropic etch in a reactive ion etching tool (RIE, from SPTS) based on SF_6 at a substrate temperature of 20 °C. The SF_6 gas flow was kept constant at 35 sccm at a process pressure of 80 mTorr. The coil power was set to 30W. This process proceeds with an extreme selectivity towards the deposited AZO without any observable harm on the prepared AZO grating structure. Controlling the etch time is crucial, since prolongation of the etching will result in a collapse of the AZO gratings. 18 min of Si etching was required to fabricate a free standing, separated AZO grating with a minimal amount of the Si core between the AZO lamellas needed to support the grating skeleton [SEM image in Figure S1d]. Note that in order to fabricate the AZO/air on AZO/Si hybrid trench structure as in Figure 1c and Figure 4 in main text, we stopped the etching process at 9 min. Since the etch rate is approximately 165nm/min, we can decide the etching depth with an accuracy of 5-10nm, which is equivalent to 2-4 seconds error in the etching time.

The fabrication procedure described here can also be used for the fabrication of dielectric trench structures made of TiO_2 and Al_2O_3 with minor changes in the process[1].

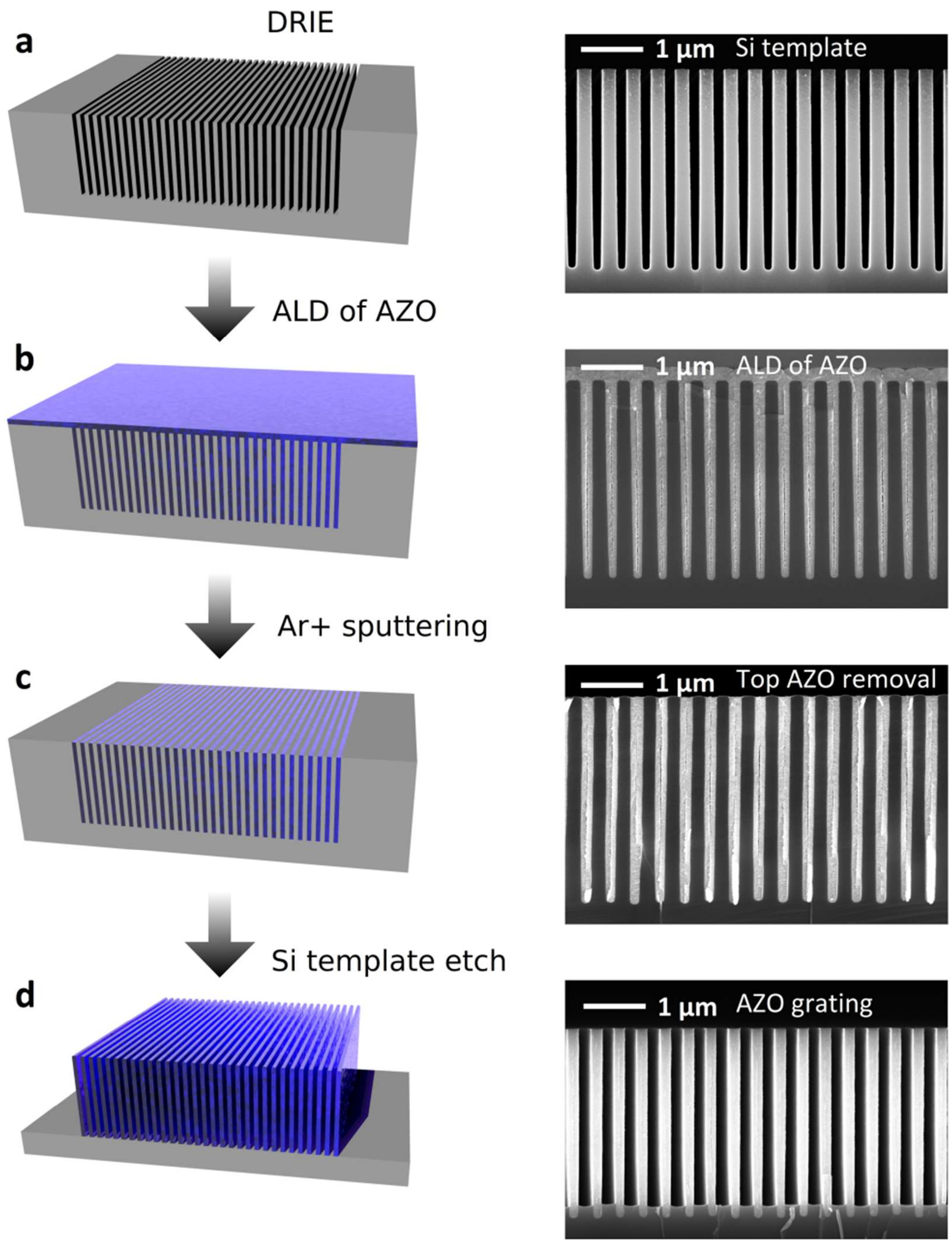

Figure S1. Schematic of AZO trench fabrication and corresponding SEM cross section image. (a) Realization of silicon template using deep reactive ion etching (DRIE, Bosch process). (b) AZO coating layer deposited by ALD on silicon template. (c) Removal of the top part of the AZO layer using physical Ar^+ ion sputtering. (d) Selective silicon etch (template removal) to fabricate free standing AZO trenches.

2. Optical characterization of hyperbolic metamaterials

The effective uniaxial permittivity tensor can be defined by $\varepsilon_x = \varepsilon_e$, $\varepsilon_y = \varepsilon_z = \varepsilon_o$ where ε_o and ε_e are the effective ordinary and extraordinary permittivities, respectively. The dielectric function of the 100 nm thick AZO film as well as the ordinary and extraordinary permittivities (ε_o and ε_e) for the trench structures in air and silicon were determined experimentally. In this regard, the intensity transfer matrix method, by which the Fabry-Perot interference fringes from the metamaterial structure or the AZO film will be retained whereas the fringes from the substrate will vanish[2], was used to calculate the normal incidence reflectance spectra of the metamaterial/substrate system. Drude-Lorentz (D-L) dielectric function was used to model the ordinary permittivity of the trench structures:

$$\varepsilon(\omega) = \varepsilon_\infty \left(1 - \frac{\omega_p^2}{\omega^2 + i\,\omega\gamma}\right) + \sum_j \frac{S_j \omega_{f,j}^2}{\omega_{f,j}^2 - \omega^2 - i\,\omega\Gamma_j}, \tag{1}$$

where ε_∞, ω_p, γ, and i are the high-frequency dielectric constant, plasma frequency, electrons plasma damping and the imaginary unit ($\sqrt{-1}$), respectively. S_j, $\omega_{f,j}$, and Γ_j are the strength, resonance frequency and damping for the jth Lorentzian oscillator, respectively. In case of the plain AZO film only the Drude part, and in case of the extraordinary permittivity of the trench structures, as well as the Si substrate, only the Lorentzian terms of the dielectric function were used.

The calculated reflectance spectra were then fitted to the reflectance spectra measured by VERTEX 70 Fourier transform infrared (FTIR) spectrometer from Bruker in order to retrieve the parameters of the dielectric functions. Measurements were done at five different points on each sample and the error bars were considered in the curve fitting algorithm which is based on the Levenberg-Marquardt method[3].

2-A. AZO film

In order to find the optical properties of the AZO film we first need to characterize the 500 μm thick double side polished (DSP) silicon substrate on top of which the films were deposited. Since the IR transmission measurements showed that the DSP Si wafers are transparent in this wavelength range, the spectrometer sample holder's mirror and the airgap below the samples had to be considered in the fitting. Five Lorentzian terms together with ε_∞

were used as the dielectric function of the Si. Figure S2a shows the measured reflectance spectrum together with the fitted curve and Table S3 shows the fitted parameters for Si. The fitted value for ε_∞ was 12.04. Figure S2b shows the real and imaginary parts of the Si permittivity. Although the dispersion of Si is very minute in this wavelength range, it affects the reflectance spectra from samples in some cases. The thickness of the airgap was also fitted and found to be around 8 μm.

Table S3. Retrieved dielectric function parameters for Si.

j	1	2	3	4	5
S_j,	0.000389	0.000618	9.81 E-5	0.000136	2.72 E-5
Γ_j [THz]	3.07	1.468	1.37	2.97	0.72
$\omega_{f,j}$ [THz]	15.24	18.32	22.396	26.69	33.18

Using the retrieved permittivity for the substrate, the curve fitting procedure was done for the 100 nm thick AZO film, considering Drude dielectric function for AZO. Figure S2c shows the measured reflectance spectrum together with the fitted curve for the AZO films and Table S4 shows the retrieved parameters of the Drude model. The dips at around 11 and 16.5 μm originate from the absorption in the Si substrate, and 9 and 13.5 μm from SiO_2 on the Si surface[4]. Figure S2d shows the permittivity of the AZO film.

Table S4. Retrieved dielectric function parameters for AZO.

γ [THz]	ω_p [THz]	ε_∞
35	147.8	3.45

2-B. AZO trench structures

In order to find ε_o and ε_e, reflectance spectra from the samples were measured at 12 ° angle of incidence using a TE-polarized light with the sample placed such that the electric field was parallel or perpendicular to the trench layers, respectively (Figure S3).

D-L dielectric function with two Lorentzian terms was used to model the ordinary permittivity of the AZO trench structure in Si (AZO/Si). Figure S4a shows the measured and fitted reflectance spectrum for this case. Figure S4b shows the real and imaginary parts of ε_o for AZO/Si structure.

Two Lorentzian terms together with ε_∞ were considered for the extraordinary permittivity of the AZO/Si trench structure. The measured reflectance spectrum together with the fitted curve are shown in Figure S4c. In this case Fabry-Perot oscillations start from 10 µm onwards.

The above-mentioned fitted dielectric functions were used as the permittivity of the 100 nm thick AZO/Si layer underneath the AZO/air trench structure in order to calculate the reflectance spectra and fit them with the measured ones. D-L dielectric function with one Lorentzian term was used to describe the ordinary permittivity of the AZO/air trench structure. Figure S4e shows the measured and fitted reflectance spectrum for this case.

Two Lorentzians together with ε_∞ were used to describe the extraordinary permittivity of the AZO/air trench structure. The measured and the fitted reflectance spectra for this case are shown in Figure S4g. The absorption dips originating from the Si substrate are observed at around 9, 11, 13.5, and 16.5 µm and the features below 3 µm are attributed to Fabry-Perot oscillations. Table S5 shows the fitted parameters of the dielectric function of the trench structures.

Table S5. Retrieved dielectric function parameters for trench structures.

	S_1	S_2	Γ_1 [THz]	Γ_2 [THz]	$\omega_{f,1}$ [THz]	$\omega_{f,2}$ [THz]	γ [THz]	ω_p [THz]	ε_∞
AZO/Si: ε_o	0.23	50.2	4.44	2.87	32.43	7.24	66.02	67.81	8.88
AZO/Si: ε_e	16.74	5.74	76.79	15.84	69.93	31.43	-	-	4.63
AZO/air: ε_o	7.18	-	103.51	-	47.2	-	16.06	84.24	1.6
AZO/air: ε_e	0.283	0.0136	40	9.05	134.63	43.17	-	-	1.24

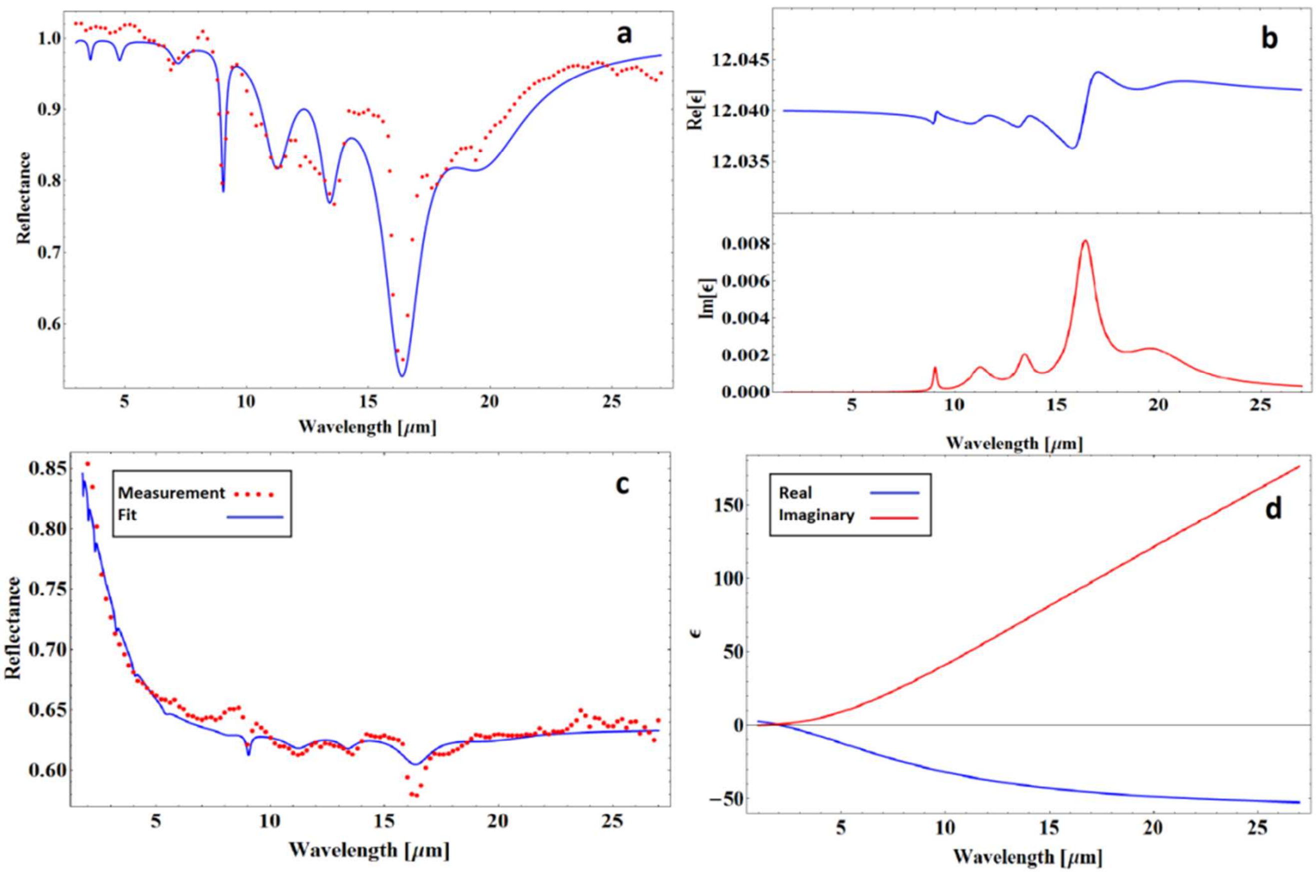

Figure S2. Optical characterization of AZO film. (a) Measured and fitted reflectance spectrum from the Si substrate. (b) Real and imaginary parts of the permittivity of the Si substrate. (c) Measured and fitted reflectance spectrum from 100 nm AZO film on DSP Si substrate. (d) Real and imaginary parts of the permittivity of the AZO film.

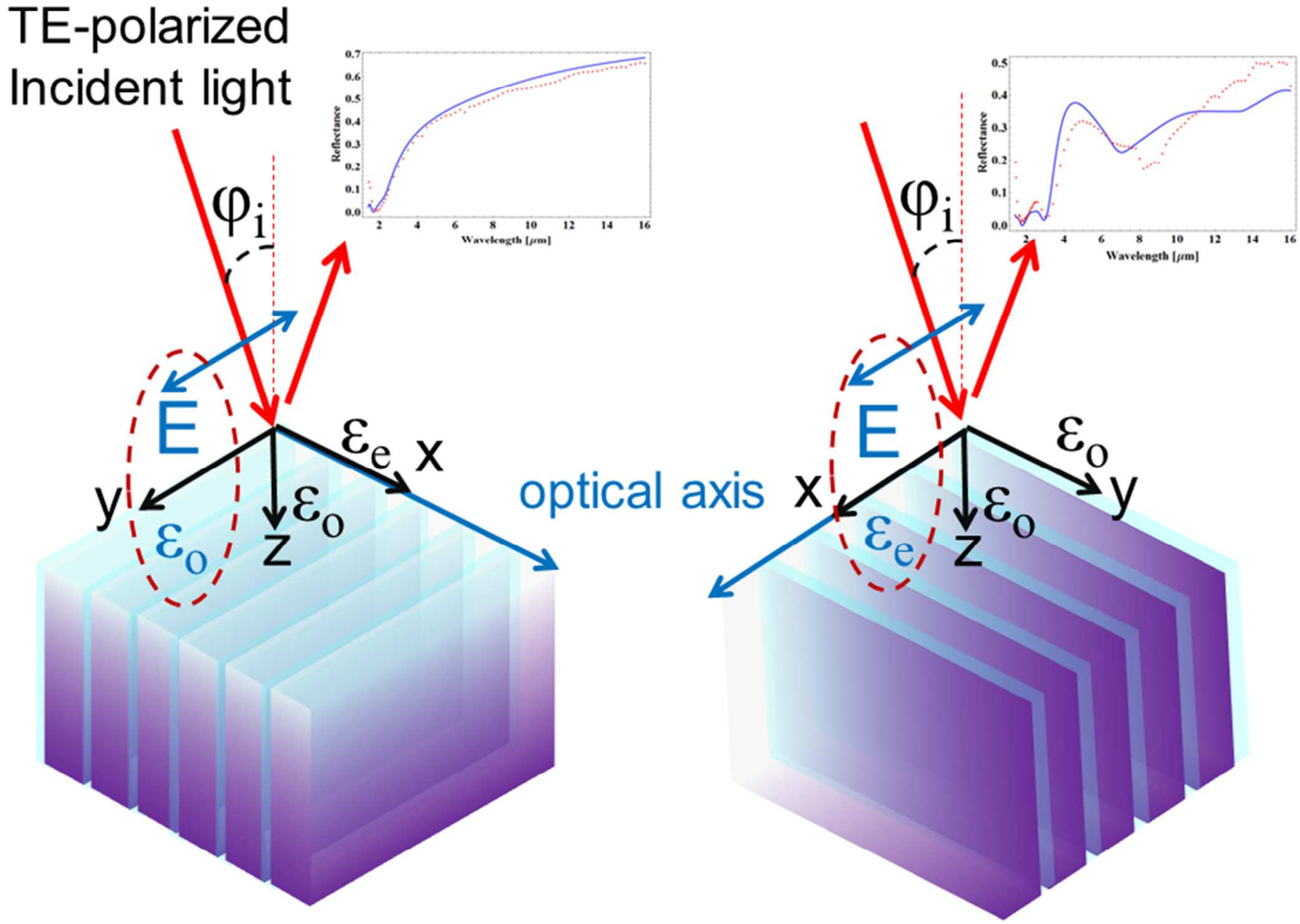

Figure S3. Orientation of the electric field with respect to the trench layers for measuring ε_o and ε_e.

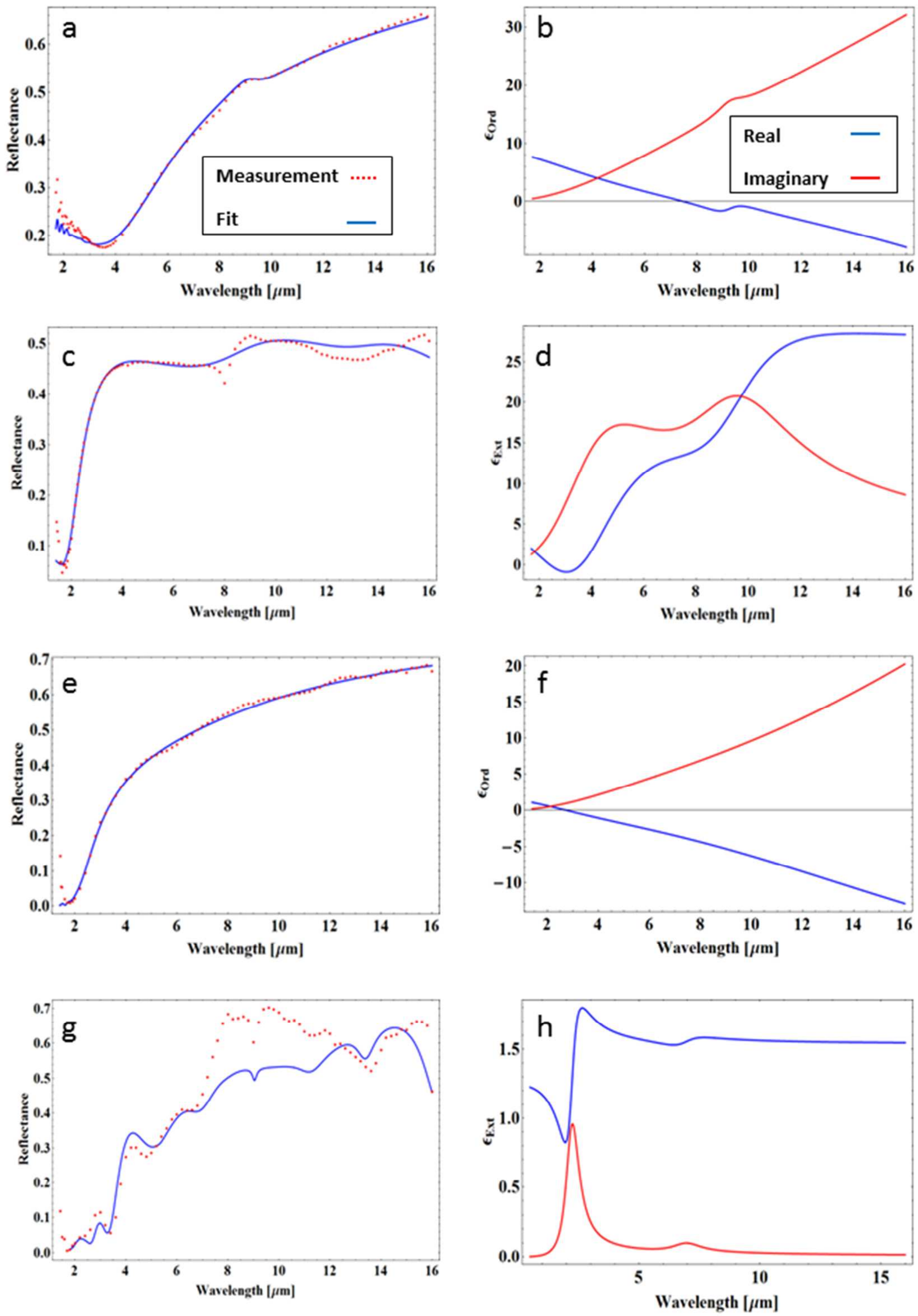

Figure S4. Measured and fitted reflectance spectra. (a) AZO/Si trench ordinary ε_o, (c) AZO/Si trench extraordinary ε_e, (e) AZO/air trench ordinary ε_o and (g) AZO/air trench extraordinary ε_e together with (b,d,f,h) their pertaining fitted permittivities.

3. Effect of airgap on reflectance maps

The reflectance maps corresponding to different airgaps are shown in Figure S5. For smaller airgaps the resonances corresponding to excitation of the modes become wider. It occurs because of increase of the radiation losses in the prism. The best matching between the experiment and simulation is achieved at the airgap 0.5μm.

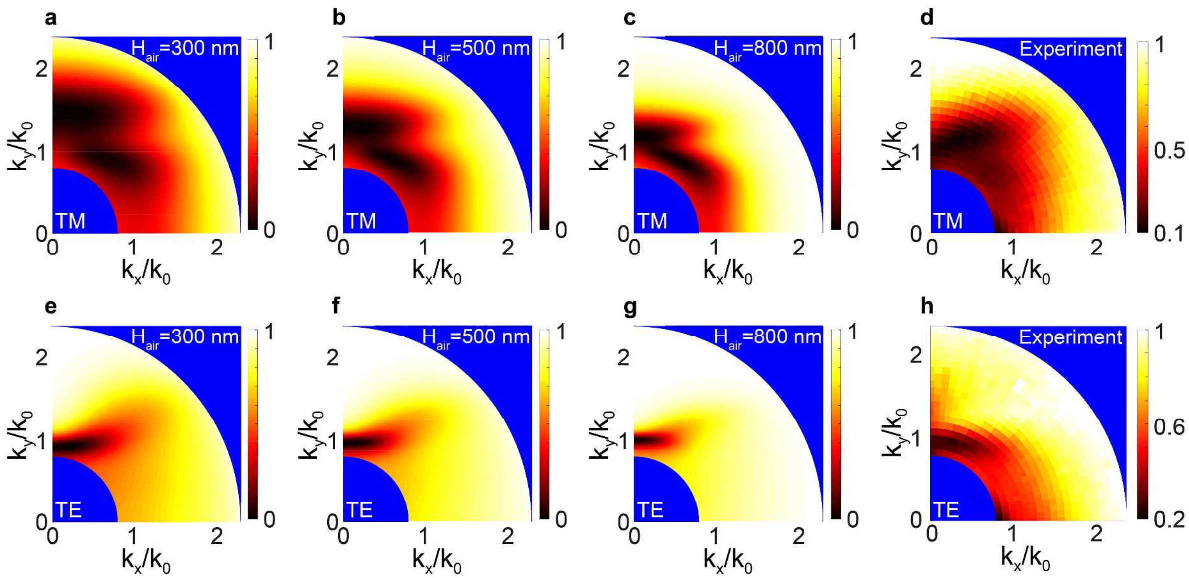

Figure S5. Influence of airgap for AZO/air trench structures. Comparison of reflectance maps calculated for different air gaps (H_{air}) between the ZnSe prism and sample with the reflectance maps obtained in the experiment for (a,e) H_{air} = 300 nm for panels, (b,f) H_{air} = 500 nm for panels, (c,g) H_{air} = 800 nm for panels and (d,h) reflectance maps obtained in the experiment. The upper row of the panels (a,b,c,d) correspond to TM polarization of the incident wave. The lower row of the panels (e,f,g,h) correspond to TE polarization of the incident wave. The wavelength of the incident wave for all panels is 6 μm. The values of the permittivities were extracted from the experiment (see Supplementary Table 5).

4. Effective medium approach vs effective parameters extracted from experiment

Figure S6a and S6b show the reflectance spectra obtained numerically using permittivities calculated from the effective medium theory and extracted from the experiment with normal incidence, respectively. It can be noted that there is only a slight quantitative difference between the two numerical approaches. Figure S5c shows the experimental reflectance map.

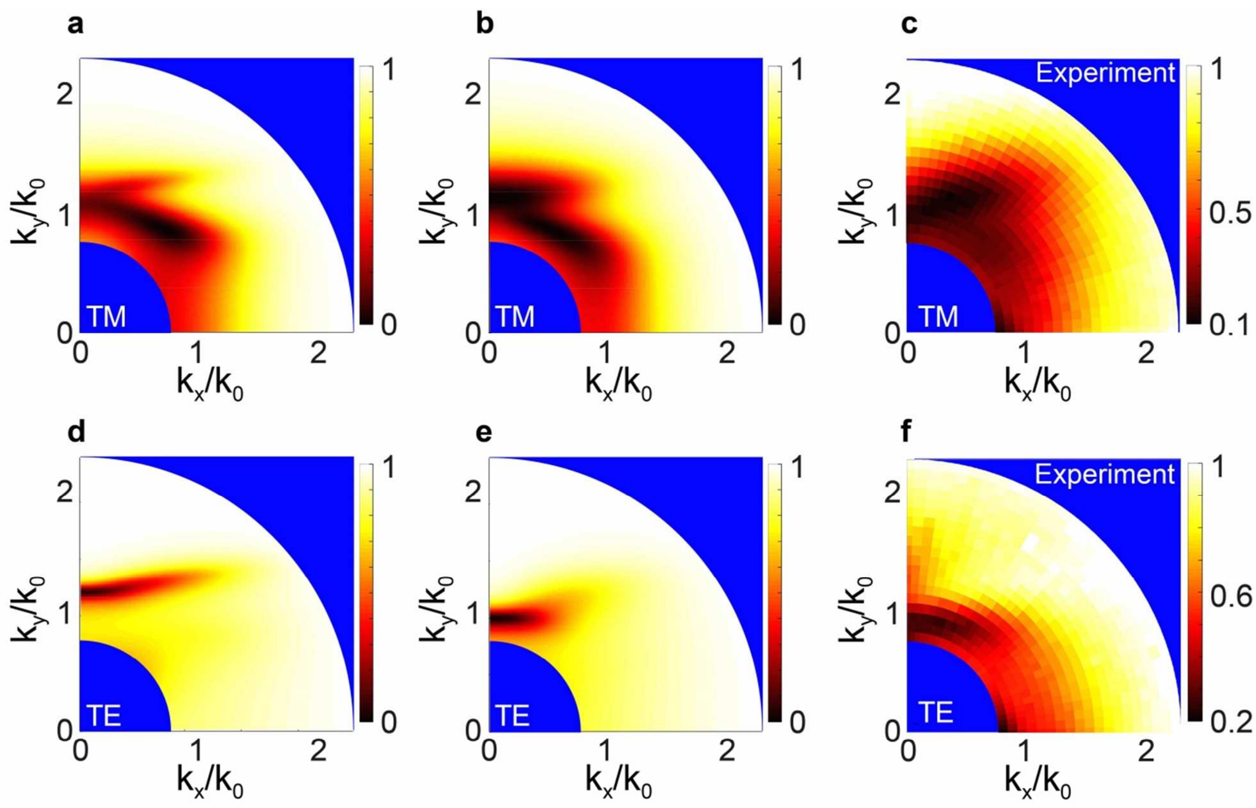

Figure S6. Effective medium approach vs effective parameters for AZO/Air trench structures. Comparison of the reflectance maps obtained numerically using permittivities (a,d) calculated within EMT and (b,e) extracted from the experiment. (c,f) Reflectance map obtained in the experiment. Panels (a,b,c) correspond to TM polarization of the incident wave. Panels (d,e,f) correspond to TE polarization of the incident wave. The wavelength of the incident wave for all panels is 6 μm. The air gap between the ZnSe prism and the sample is H_{air} = 500 nm.

5. Bi-slab model vs full-wave simulations

Figure S7 shows reflectance maps calculated using full-wave simulations (Comsol Multiphysics)[5] and a bi-slab model where the trench structures are considered as homogeneous anisotropic materials. It can be noticed that the bi-slab model provides a good description of the structure for different levels of silicon in the trenches.

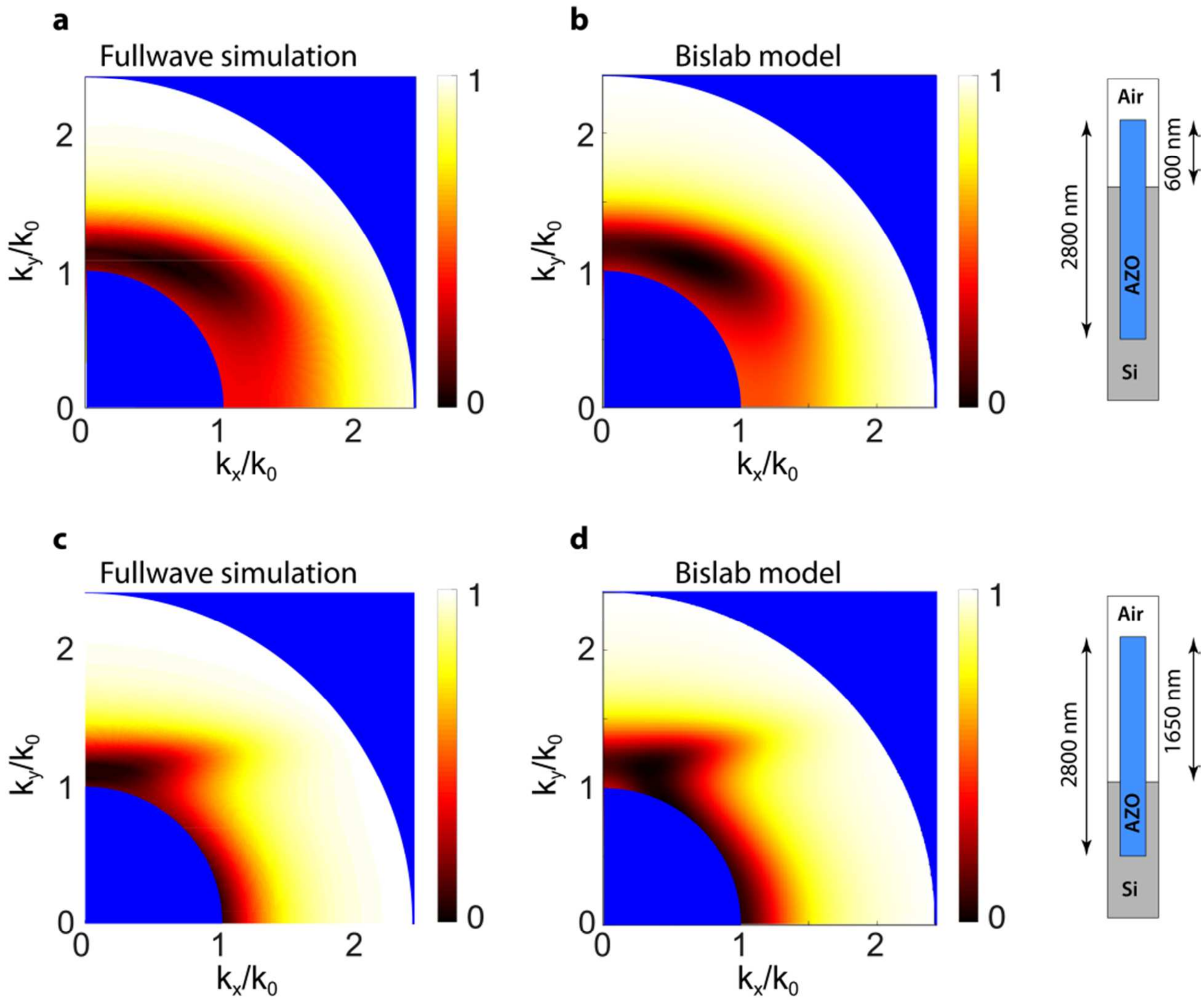

Figure S7. Hybrid trench structures. Comparison of the reflectance maps obtained using (a,c) fullwave numerical simulation with ones (b,d) obtained using the transfer matrix method (bislab model). The upper row of the panels (a,b) correspond to TE polarization of the incident wave. The lower row of the panels (c,d) correspond to TM polarization of the incident wave. The wavelength of the incident wave for all panels is 6 μm.

6. Experimental results

Our experimental setup is based on an Otto configuration mounted on the FTIR spectrometer (VERTEX 70, Bruker). A hemispherical ZnSe prism (25.4mm diameter) is placed on the sample with an air gap between the ZnSe prism and the trench structures. The measurement was conducted for the wavelength range of λ = 2.0 – 16.0 µm. The input light is a linearly-polarized beam (TM polarization, magnetic field in x-y plane or TE polarization, electric field in x-y plane) obtained by a polarizer and is focused on the surface of the structure through the ZnSe prism. We measured a series of normalized reflectance spectra at each angle from optical axis θ and incident angle φ_i. The beam has incident angle of φ_i and is manually controlled using a goniometer with the increment of each 3 º from φ_i = 20 º - 74 º for AZO/air structures as shown in Figure S8. For AZO/Si and hybrid bi-layer AZO/air + AZO/Si structures, measurements were conducted with an increment of 2 º from φ_i = 24 º - 60 º as shown in Figure S8 - 13. The divergence angle of the input beam is $\Delta\varphi_i$ = ± 1.7 º. The crystal orientation relative to the incident beam is controlled by an increment of 3 º from θ = 0 º - 90 º for all cases. The reflectance is normalized to the reflectance at θ = 90 º and φ_i = 74 º for all cases. To plot the figures in the k-space, the dispersion of the ZnSe prism is taken into account based on the spectral dependencies of the refractive index[6].

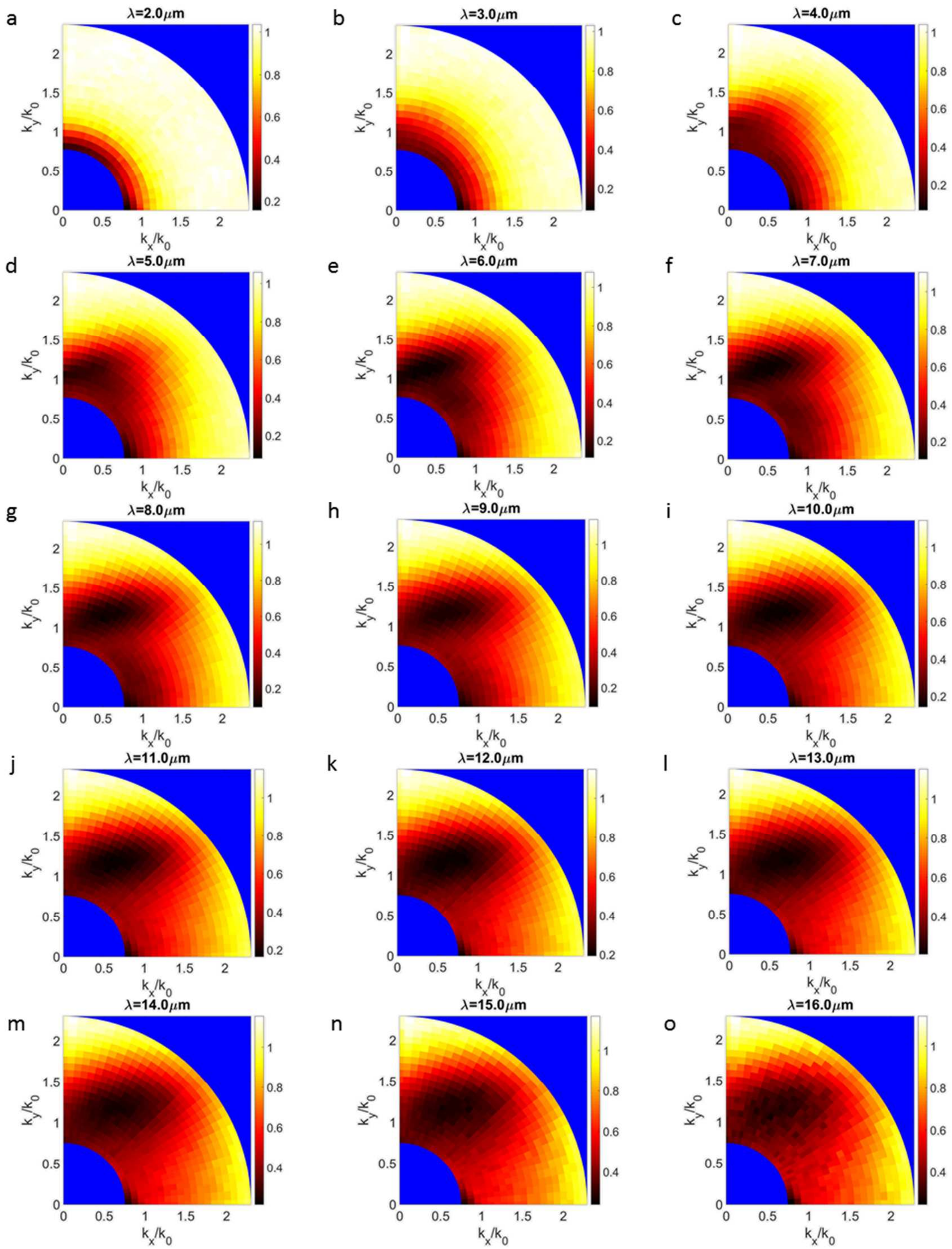

Figure S8. Experimental reflection in k-space for AZO/air trench structure for TM-polarized incident light. (a) λ = 2.0 μm, (b) 3.0 μm, (c) 4.0 μm, (d) 5.0 μm, (e) 6.0 μm, (f) 7.0 μm, (g) 8.0 μm, (h) 9.0 μm, (i) 10.0 μm, (j) 11.0 μm, (k) 12.0 μm, (l) 13.0 μm, (m) 14.0 μm, (n) 15.0 μm, and (o) 16.0 μm. The Otto-configuration consists of ZnSe prism, airgap, AZO/air trench structure, thin AZO/Si trench structure, and Si substrate. The AZO/air trench metamaterial with height L = 3.2 μm on AZO/Si trenches with height $H - L$ = 0.1 μm.

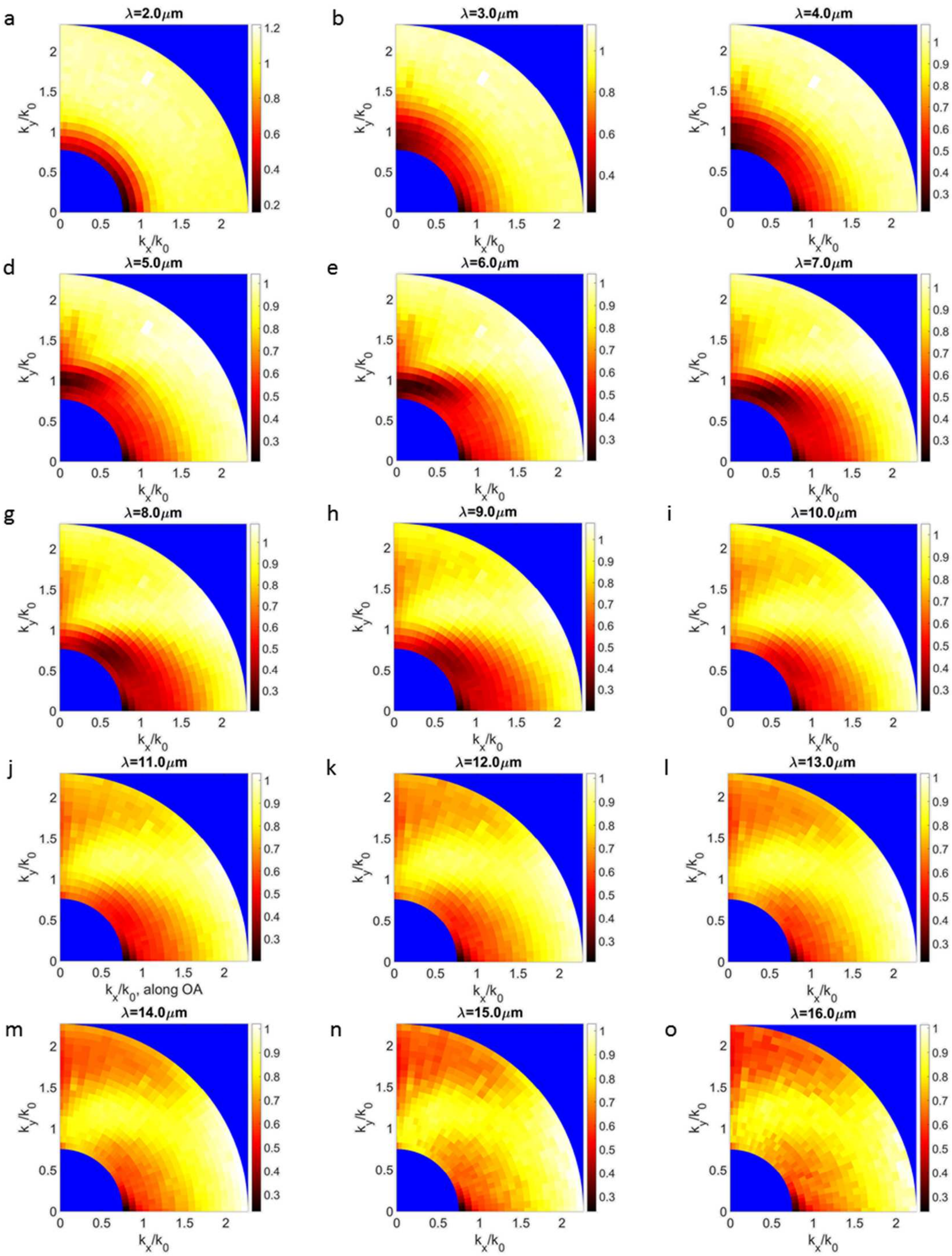

Figure S9. Experimental reflection in k-space for AZO/air trench structure for TE-polarized incident light. (a) λ = 2.0 μm, (b) 3.0 μm, (c) 4.0 μm, (d) 5.0 μm, (e) 6.0 μm, (f) 7.0 μm, (g) 8.0 μm, (h) 9.0 μm, (i) 10.0 μm, (j) 11.0 μm, (k) 12.0 μm, (l) 13.0 μm, (m) 14.0 μm, (n) 15.0 μm, and (o) 16.0 μm. The Otto-configuration consists of ZnSe prism, airgap, AZO/air trench structure, thin AZO/Si trench structure, and Si substrate. The AZO/air trench metamaterial with height L = 3.2 μm on AZO/Si trenches with height $H - L$ = 0.1 μm.

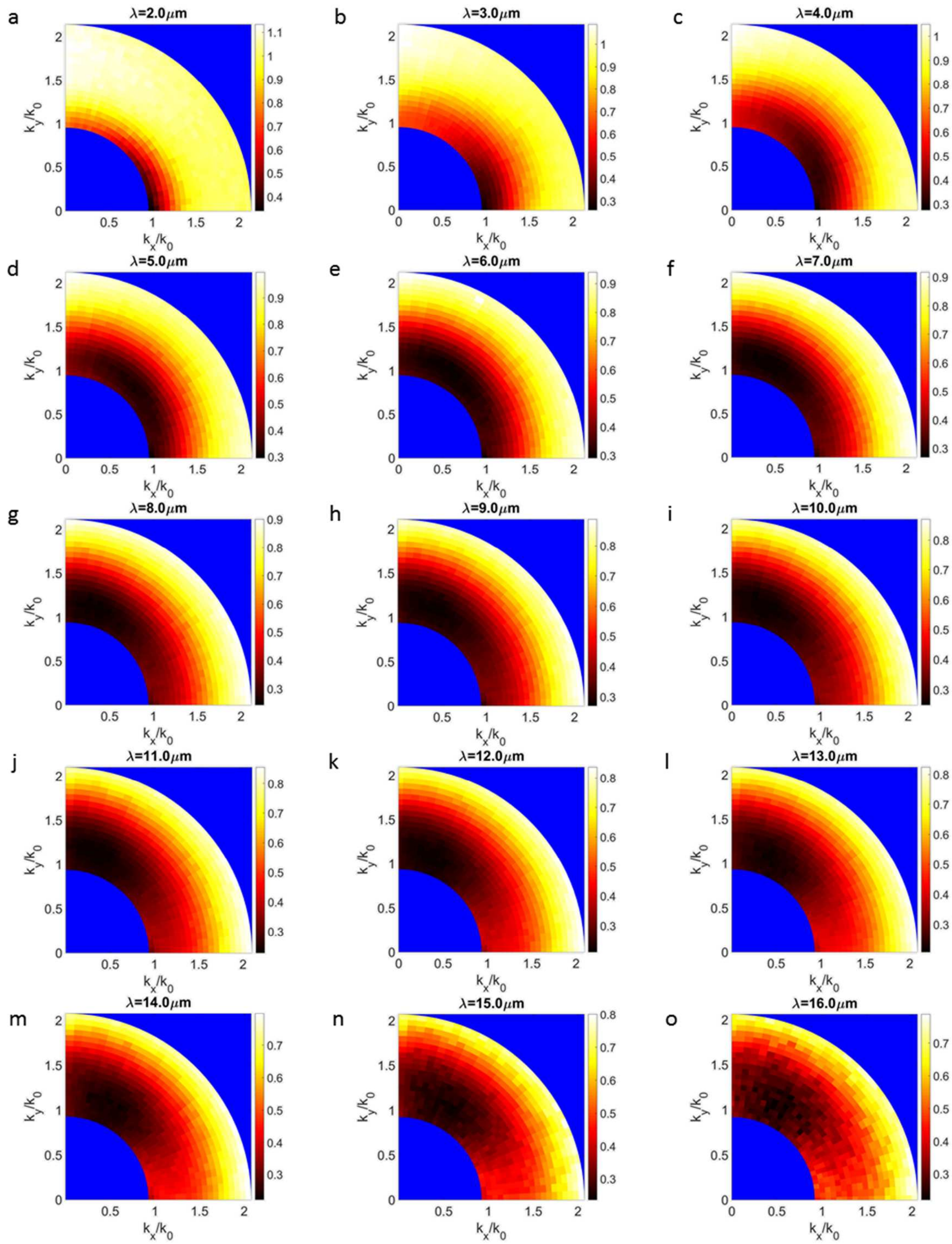

Figure S10. Experimental reflection in k-space for AZO/Si trench structure for TM-polarized incident light. (a) λ = 2.0 μm, (b) 3.0 μm, (c) 4.0 μm, (d) 5.0 μm, (e) 6.0 μm, (f) 7.0 μm, (g) 8.0 μm, (h) 9.0 μm, (i) 10.0 μm, (j) 11.0 μm, (k) 12.0 μm, (l) 13.0 μm, (m) 14.0 μm, (n) 15.0 μm, and (o) 16.0 μm. The Otto-configuration consists of ZnSe prism, airgap, AZO/Si trench structure, and Si substrate. The AZO/Si trenches has height $H - L$ = 2.8 μm.

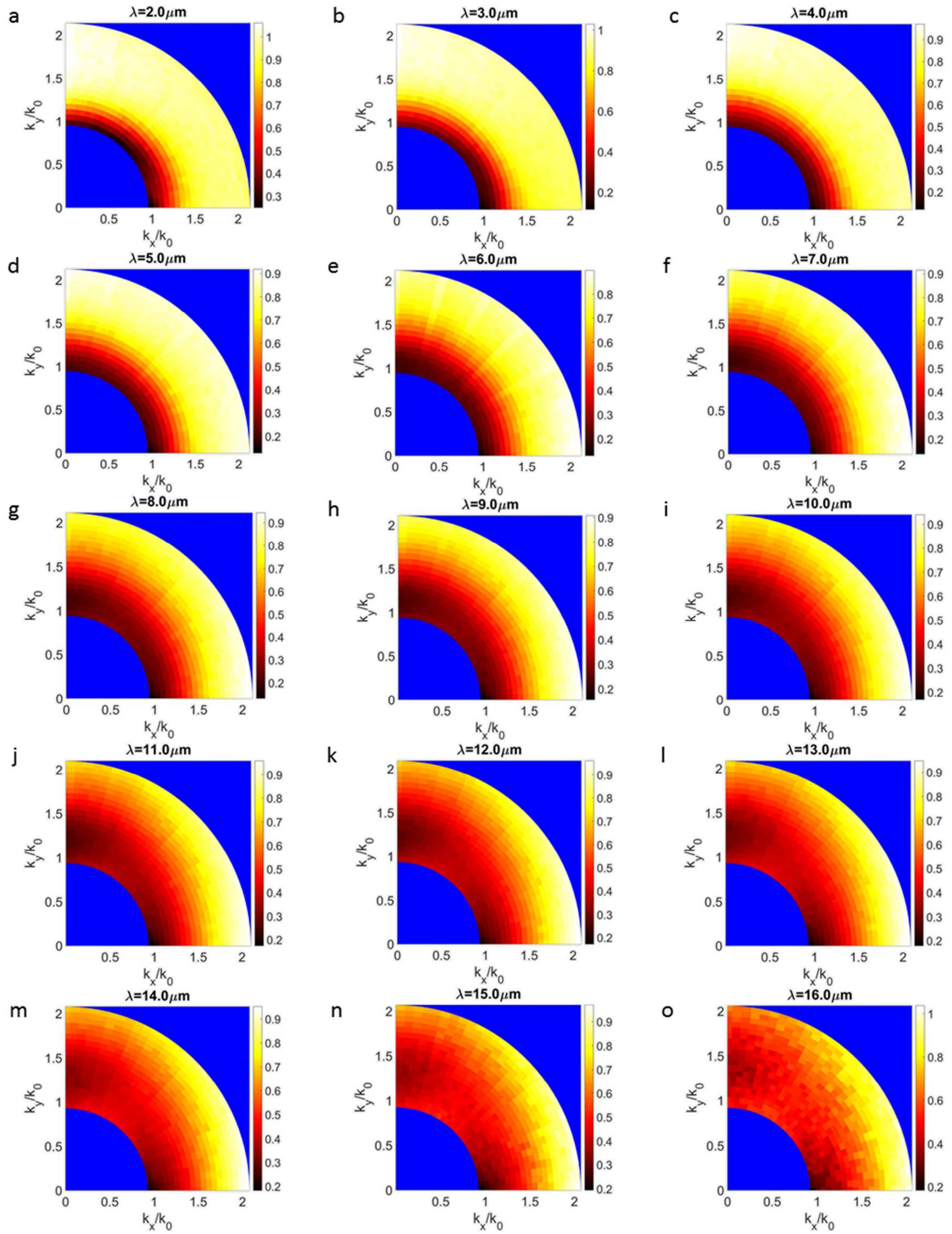

Figure S11. Experimental reflection in k-space for AZO/Si trench structure for TE-polarized incident light. (a) λ = 2.0 μm, (b) 3.0 μm, (c) 4.0 μm, (d) 5.0 μm, (e) 6.0 μm, (f) 7.0 μm, (g) 8.0 μm, (h) 9.0 μm, (i) 10.0 μm, (j) 11.0 μm, (k) 12.0 μm, (l) 13.0 μm, (m) 14.0 μm, (n) 15.0 μm, and (o) 16.0 μm. The Otto-configuration consists of ZnSe prism, airgap, AZO/Si trench structure, and Si substrate. The AZO/Si trenches has height $H - L$ = 2.8 μm.

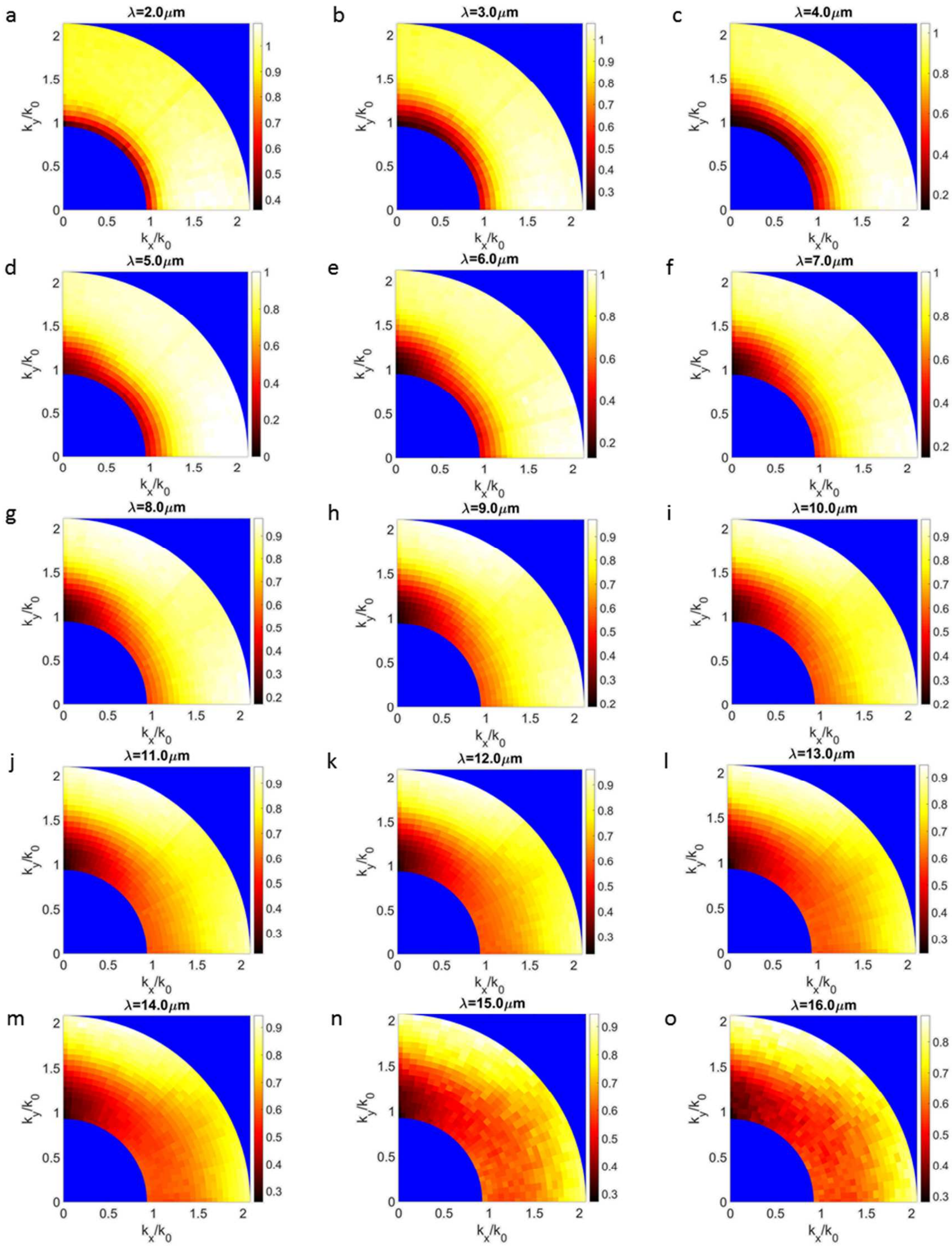

Figure S12. Experimental reflection in k-space for AZO/air+Si trench structure for TM-polarized incident light. (a) λ = 2.0 μm, (b) 3.0 μm, (c) 4.0 μm, (d) 5.0 μm, (e) 6.0 μm, (f) 7.0 μm, (g) 8.0 μm, (h) 9.0 μm, (i) 10.0 μm, (j) 11.0 μm, (k) 12.0 μm, (l) 13.0 μm, (m) 14.0 μm, (n) 15.0 μm, and (o) 16.0 μm. The Otto-configuration consists of ZnSe prism, airgap, AZO/air trench structure (L = 1.65 μm), AZO/Si trench structure ($H - L$ = 1.15 μm), and Si substrate.

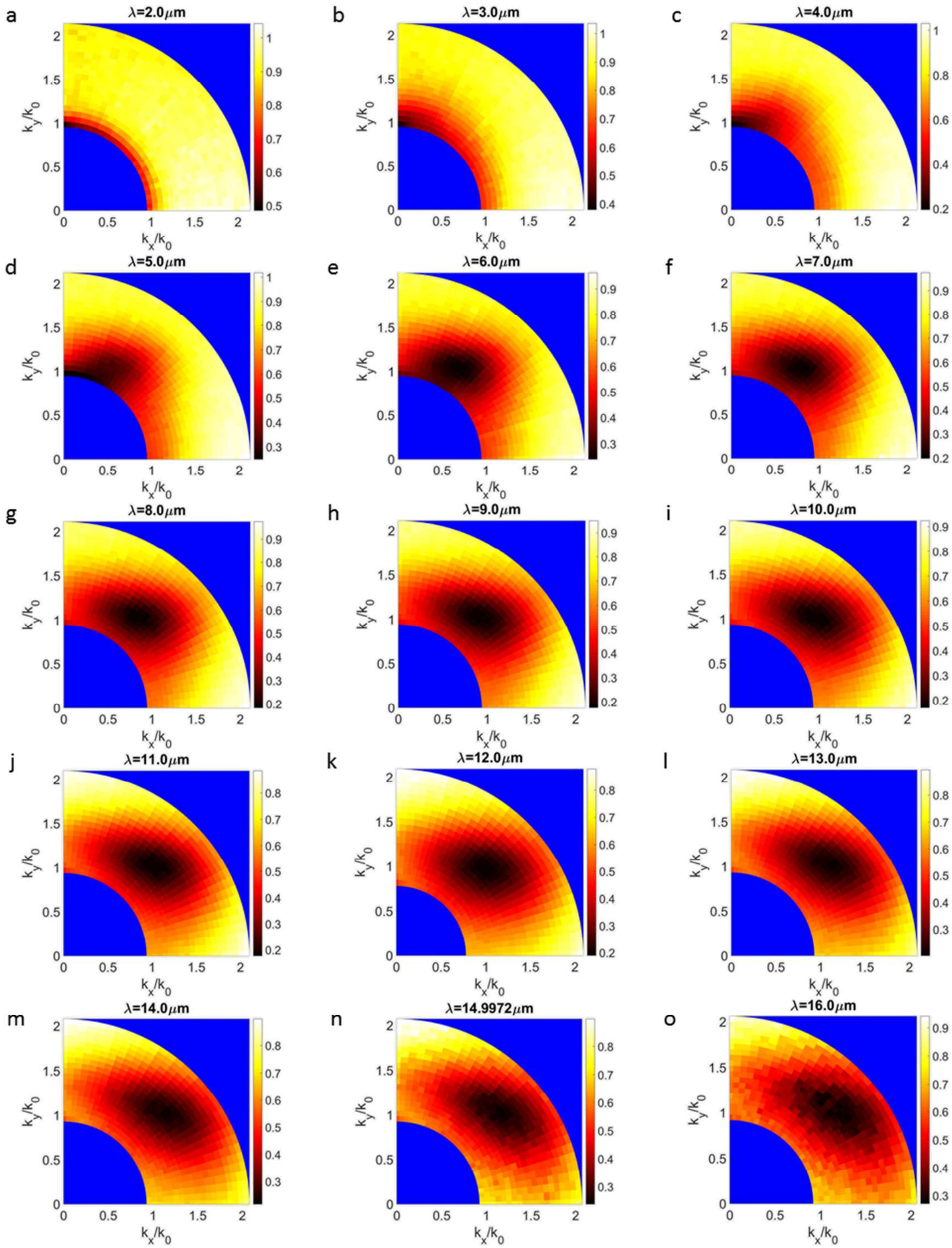

Figure S13. Experimental reflection in k-space for AZO/air+Si trench structure for TE-polarized incident light. (a) λ = 2.0 μm, (b) 3.0 μm, (c) 4.0 μm, (d) 5.0 μm, (e) 6.0 μm, (f) 7.0 μm, (g) 8.0 μm, (h) 9.0 μm, (i) 10.0 μm, (j) 11.0 μm, (k) 12.0 μm, (l) 13.0 μm, (m) 14.0 μm, (n) 15.0 μm, and (o) 16.0 μm. The Otto-configuration consists of ZnSe prism, airgap, AZO/air trench structure (L = 1.65 μm), AZO/Si trench structure ($H - L$ = 1.15 μm), and Si substrate.

REFERENCES

(1) Shkondin. E. *et al. Journal of Vacuum Science & Technology A* **2016**, 34, 031605.

(2) Gabriel, C. J.; Nedoluha, A. *Opt. Acta*, **1971**, 18, 415.

(3) Press, W. H.; Flannery, B. P.; Teukolsky, S. A.; Vetterling, W. T. *Numerical Recipes*; Cambridge University Press: Cambridge, England, 1986.

(4) Kitamura, R.; Pilon, L.; Jonasz, M. *Appl. Opt.* **2007**, 46, 8118.

(5) COMSOL Multiphysics® v. 5.0. www.comsol.com. COMSOL AB, Stockholm, Sweden.

(6) Connolly, J.; DiBenedetto, B.; Donadio, R. *Proc. SPIE*, **1979**, 181, 141.